Association of Hydrophobically End-Capped Poly(ethylene oxide)

Christophe Chassenieux, Taco Nicolai, and Dominique Durand*

Chimie et Physique des Matériaux Polymères, UMR CNRS, Université du Maine, BP 535, 72017 Le Mans Cedex, France

Received March 14, 1997; Revised Manuscript Received June 3, 1997[⊗]

ABSTRACT: The associative character of poly(ethylene oxide) (PEO) end-capped with dodecyl groups was studied by using static and dynamic light scattering and viscometry. The effect of functionalization is investigated by comparing results on unmodified PEO with PEO of the same molar mass end-capped at one or both ends. The molar mass dependence is investigated by comparing difunctionalized PEO samples with different molar masses: 10, 20, and 35 kg/mol. The experimental data are well described by a crude model which assumes open association and incorporates interparticle interaction.

Introduction

Over the last decade, associative polymers have attracted widespread interest both from a theoretical and experimental point of view. Associative polymers contain a small amount of functional groups which associate into multiplets in the melt or in solution.

Hydrophobically end-capped poly(ethylene oxide) (PEO) belongs to this family and has industrial importance, e.g., as a modifier of rheological properties or as an oil-recovery agent. Most of the industrial products are ethylene oxide−urethane copolymers (HEUR) obtained by a condensation reaction. The large polydispersity and the presence of urethane groups in such systems may influence the association phenomena.[1] For this reason new synthesis methods have been developed to obtain model systems, i.e., without urethane groups and with small polydispersity.[2]

Properties of aqueous solutions of PEO end-capped with alkyl groups have been studied by several techniques. The critical association concentration (CAC) has been measured by fluorescence spectroscopy[2−4] and was found to increase with increasing molar mass. Above CAC the viscosity increases more sharply with increasing concentration than unfunctionalized PEO.[2−3] An estimate of the number of end groups per multiplet has been obtained from quenching fluorescence measurements.[3] The concentration dependence of the self-diffusion coefficient has been measured by NMR.[4−6]

Here we present results of a study on aqueous solutions of monodisperse PEO containing dodecyl groups on one or both ends. We compare dynamic (DLS) and static (SLS) light scattering and viscosity measurements on the same solutions and we look at the effect of molar mass by comparing model polymers with molar mass 10, 20, and 35 kg/mol. We are able to model the SLS and DLS results assuming open association and incorporating interactions. Our experimental results are in agreement with earlier DLS experiments on one sample reported in the literature.[3]

Experimental Section

Materials. Commercial PEO's (Hoechst) with different molar masses were purified and functionalized at one (ω) or both ends (α,ω) with dodecyl groups by J. François and co-workers in Strasbourg, using a method reported elsewhere.[2] The degree of substitution of the hydroxyl groups was determined by nuclear magnetic resonance and was found to range from 85% to 100%. The polydispersity of the unmodified polymers was determined by size exclusion chromatography (SEC) (see Table 1).

Light Scattering. DLS and SLS measurements were done by using an ALV-5000 multibit, multitau full digital correlator in combination with a Malvern goniometer and an Ar-ion laser emitting vertically polarized light with a wavelength (λ) of 488 nm. The time range investigated is between 0.2 μs and a few seconds. The angular dependence of the light scattered by water is less than 1% over the angle range used in this study (30°−150°).

The refractive index increment of modified PEO in water has been measured by Jeanne François and co-workers[7] and is equal to 0.14 mL/g which is close to the value for nonmodified PEO.

All measurements were done at 20 ± 1°C unless otherwise specified.

The intensity autocorrelation functions $g_2(t)$ obtained from DLS were analyzed in terms of a continuous distribution of relaxation times:

$$g_1(t) = \int_0^\infty A(\tau) \exp(-t/\tau)\, d\tau \qquad (1)$$

Here $g_1(t)$ is the normalized electric field autocorrelation function related to $g_2(t)$ via the so-called Siegert relation.[8] The REPES routine was used to obtain $A(\tau)$ without assuming a specific shape.[9]

Viscometry. Viscosity measurements were done in the linear response regime using two types of viscometers, depending on the concentration. At low concentrations, a low-shear Couette flow rheometer, Contraves LS40, was used, while at high concentrations we used the Haake RS100 rheometer with cone-plate geometry. All measurements were done at 20 ± 1 °C unless otherwise specified.

Sample Preparation. All solutions were prepared in freshly distilled water with 200 ppm/L sodium azoture added as a bacteriostatic agent. Solutions of unfunctionalized PEO used as precursors for the functionalized samples contained a small amount of large aggregates. The aggregates were removed by filtration through 0.2 μm pore size Anotope filters. The effect of filtration on the relaxation time distribution obtained from DLS is illustrated in Figure 1. Before filtration, correlation functions are characterized by two relaxation processes. The slow relaxation process is due to diffusion of large PEO aggregates and can be eliminated by filtration. The aggregation of PEO chains is thought to be induced by hydrophobic impurities in the sample.[10] The average relaxation time of the fast process is not influenced by these spurious aggregate and remains the same before and after filtration. The viscosity of the sample is not influenced, as it remains the same before and after filtration.

Solutions of modified PEO are very viscous at high concentrations, which renders filtration impossible. For more dilute samples, the filtration leads to the formation of air bubbles which are stabilized by the modified PEO, which acts as a surfactant. For these reasons we have chosen not to filter

* To whom correspondence should be addressed.
[⊗] Abstract published in *Advance ACS Abstracts,* July 15, 1997.

S0024-9297(97)00354-9 CCC: $14.00 © 1997 American Chemical Society

Table 1. Characteristics of the Unmodified PEO Samples

sample	M_w/M_n[a]	M_w,[b] kg/mol	$M_wA_2 \times 10^3$ L/g	R_h nm	$k_d \times 10^3$ L/g	R_g,[c] nm	C^*,[d] g/L	C^*,[e] g/L
PEO35	1.1	34.0 ± 2	97 ± 10	6.1 ± 0.2	28 ± 2	9.4	16	10
PEO20	1.02	18.8 ± 0.7	47 ± 6	4.2 ± 0.1	12 ± 1	6.7	25	22
PEO10	1.03	8.7 ± 0.5	24 ± 2	2.7 ± 0.1	8 ± 1	4.2	45	41

[a] Obtained from SEC by J. François et al.[3,4] [b] Measured by static light scattering. [c] calculated from the relation $R_g = 0.215M^{0.583}$ given in ref 12. [d] Using $C^* = 3M_w/(4\pi R_g^3 Na)$. [e] Using $C^* = 1/(M_wA_2)$.

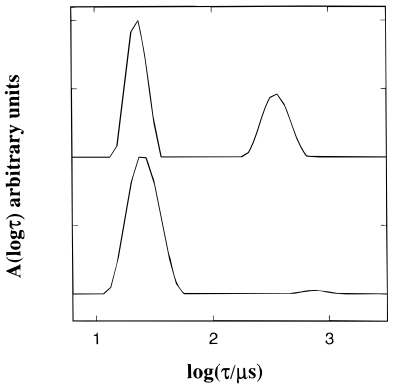

Figure 1. Relaxation time distributions obtained from DLS for PEO35 at $C = 10$ g/L and $\theta = 150°$, before (top) and after filtration (bottom).

solutions of modified PEO and instead to correct for the contribution of PEO aggregates to the total scattered intensity, as described below.

Results

Unfunctionalized PEO. We investigated solutions of unfunctionalized PEO samples with three different molar masses using SLS, DLS, and viscometry.

SLS. For weakly interacting systems, the excess scattering intensity ($I - I_{sol}$) extrapolated to zero scattering angle is related to the weight-average molar mass of the particle (M_w) and the second virial coefficient A_2:[11]

$$\frac{KC}{R_0} = \frac{1}{M_w} + 2A_2C \tag{2}$$

where $R_0 \propto (I - I_{sol})_{\theta\to 0}$ is the Rayleigh ratio extrapolated to zero scattering angle (θ) and K is a contrast factor which depends on the refractive index increment. We have used toluene as a reference with $R_{tol} = 4.0 \times 10^{-5}$ cm^{-1}. Values of M_w and A_2 are listed in Table 1 and agree with literature data.[12]

The concentration dependence of KC/R_0 is shown in Figure 2. The values of KC/R_0 are normalized by M_w and the concentration is normalized by the critical overlap concentration, C^*, defined as $C^* = 3M/(4\pi R_g^3 N_a)$, where R_g is the radius of gyration and N_a is Avogadro's constant. In this representation, data from samples with different molar masses are expected to superimpose.[13] The values of R_g are too small to measure accurately by SLS, so we have used the relation between the molar mass and R_g given in ref 12. An alternative definition of the overlap concentration, $C^* = (MA_2)^{-1}$, gives similar values, see Table 1.

In the semidilute regime, i.e., for large values of C/C^*, $KC/R)_0$ is expected to have a power law dependence on C: $KC/R_0 \propto C^{1.3}$.[13] It is possible to fit the data over the whole concentration range with the following simple empirical expression, which has the expected behavior at large C/C^*:

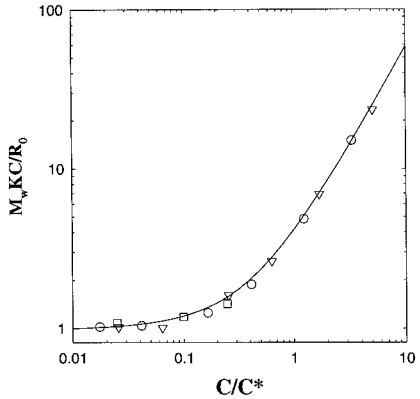

Figure 2. Variation with the reduced concentration C/C^* of KC/R_0 normalized by the weight average molar mass for PEO35 (triangles), PEO20 (circles), and PEO10 (squares). The solid line represents F_s, given by eq 3.

$$F_s = \left(1 + a_s\left(\frac{C}{C^*}\right) + b_s\left(\frac{C}{C^*}\right)^2\right)^{1.3/2} \tag{3}$$

with $a_s = 3.1 \pm 0.6$ and $b_s = 5.0 \pm 0.3$; see solid line in Figure 2.

DLS. Correlation functions measured on filtered solutions are characterized by a single peaked relaxation time distribution. The average relaxation times are q^2-dependent and can be used to calculate an apparent diffusion coefficient $D = (q^2\tau)^{-1}$, where q is the scattering wave vector defined as $q = (4\pi n/\lambda)\sin(\theta/2)$ with n the refractive index of the solvent. The initial concentration dependence of D is given by

$$D = D_0(1 + k_dC) \tag{4}$$

where D_0 is the translation diffusion coefficient extrapolated to zero concentration and k_d is the dynamic second virial coefficient. The hydrodynamic radius, R_h, can be calculated by using the Stokes−Einstein relation: $D_0 = kT/6\pi\eta_0 R_h$, with η_0 the solvent viscosity, k Boltzmann's constant, and T the absolute temperature. Measured values of R_h an k_d are given in Table 1 and are in agreement with literature data.[12]

In Figure 3, D normalized by D_0 is plotted versus the ratio C/C^*. In this representation data from samples with different molar masses superimpose.[13] It is again possible to fit all experimental data with a simple empirical expression which has the expected behavior at large C/C^*:[13]

$$F_d = \left(1 + a_d\left(\frac{C}{C^*}\right) + b_d\left(\frac{C}{C^*}\right)^2\right)^{0.7/2} \tag{5}$$

with $a_d = 1.5 \pm 0.2$ and $b_d = 0.27 \pm 0.08$

Viscosity. The viscosity normalized by the solvent viscosity is plotted as a function of C/C^* in Figure 4. In this representation, data from samples with different molar masses superimpose if the molar mass is larger than the critical molar mass for entanglement,[14] which is about 1.7 kg/mol for PEO.[15] The solid line in figure 4 represents the following empirical expression, which

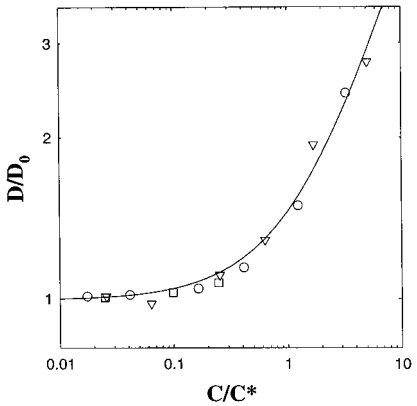

Figure 3. Variation of the normalized apparent diffusion coefficient D/D_0 with the reduced concentration C/C^* for PEO35 (triangles), PEO20 (circles), and PEO10 (squares). The solid line represents F_d, given by eq 5.

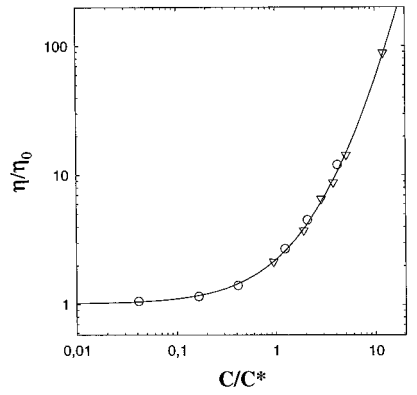

Figure 4. Variation of the viscosity η normalized by the solvent viscosity η_0 with the reduced concentration C/C^* for PEO35 (triangles) and PEO20 (circles). The solid line represents F_v, given by eq 6.

has the expected behavior at large C/C^*:[14]

$$F_v = \left(1 + a_v\left(\frac{C}{C^*}\right) + b_v\left(\frac{C}{C^*}\right)^2\right)^{15/8} \qquad (6)$$

with $a_v = 0.5 \pm 0.04$ and $b_v = 0.026 \pm 0.001$

Effect of Functionalization. We have investigated the effect of incorporation of a dodecyl group on one (ω-PEO) or both ends (α,ω-PEO) of the sample PEO20. As explained in the Experimental Section, we did not filter solutions of modified PEO so that we need to correct the light scattering results for the presence of spurious aggregates. Measurements on unfunctionalized PEO showed that the effect of these spurious aggregates on the viscosity is negligible.

The contribution of spurious aggregates at different concentrations of (α,ω-PEO) is clearly seen in the relaxation time distributions obtained from DLS; see Figure 5. The relaxation time distributions are characterized by two q^2-dependent relaxation processes over the whole concentration range. The relative amplitude of the slow mode increases with increasing concentration and decreasing q. The relaxation time of the slow mode increases strongly with increasing concentration for $C > 30$ g/L, as already observed by Alami et al.[3] for the same sample. We attribute the slow mode to diffusion of spurious aggregates present in nonfiltered solutions of modified and unmodified PEO. The strong increase of the relaxation time at $C > 30$ g/L coincides with the strong increase of the macroscopic viscosity. After correction by the macroscopic viscosity of the

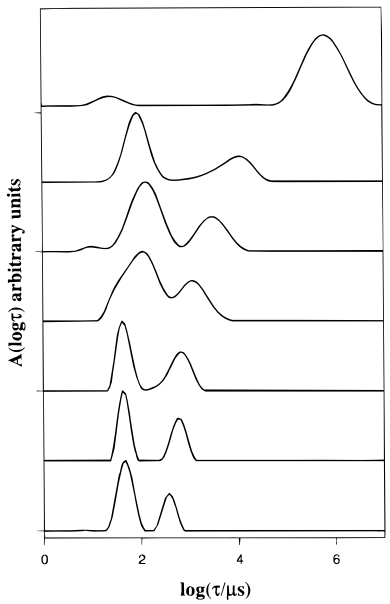

Figure 5. Relaxation time distributions obtained from DLS at different concentrations of α,ω-PEO20. From bottom to top $C = 1$, 5, 10, 20, 30, 40, and 100 g/l.

solutions, the diffusion coefficient decreases weakly with increasing concentration but is the same regardless the functionality of the sample. This means that the size of the spurious aggregates increases weakly with increasing PEO concentration.

The concentration before and after filtration of PEO solutions is the same within experimental error, which means that the PEO fraction involved in the spurious aggregates is negligible. However, the contribution to the scattering intensity can be large because it is weighed by the large molar mass of the spurious aggregates. The amplitudes of the slow, $A_s(q)$, and the fast, $A_f(q)$, mode represent the relative contribution to the scattering intensity of the spurious aggregates and of the system, respectively. We are interested in the scattering intensity of the latter given by

$$I_f(q) = \frac{A_f(q)}{A_f(q) + A_s(q)}(I - I_{sol}) \qquad (7)$$

In the following we will only consider the diffusion coefficient and the scattering intensity of the fast mode, i.e., of the system without spurious aggregates.

Viscosity. In Figure 6 the concentration dependence of the normalized viscosity is shown for α,ω-PEO20, ω-PEO20, and PEO20. For $C > 20$g/L, the increase of the viscosity is stronger for functionalized PEO, which demonstrates its associative character. As expected α,ω-PEO20 shows the strongest increase and has an almost 40 times higher viscosity than the unmodified PEO at the highest concentration investigated (100 g/L). The increase of viscosity is smaller for ω-PEO20 because only small micellelike aggregates are formed (see discussion section). The normalized viscosity does not depend on the temperature in the range investigated (5−50 °C).

SLS. In Figure 7 normalized values of KC/R_0 are plotted versus the concentration for the α,ω-PEO20, ω-PEO20, and PEO20. At low concentrations KC/R_0 equals the inverse of the molar mass of the individual PEO chains, which is 20, 22, and 19 kg/mol for α,ω-PEO20, ω-PEO20, and PEO20, respectively. The concentration dependence for ω-PEO20 and PEO20 is

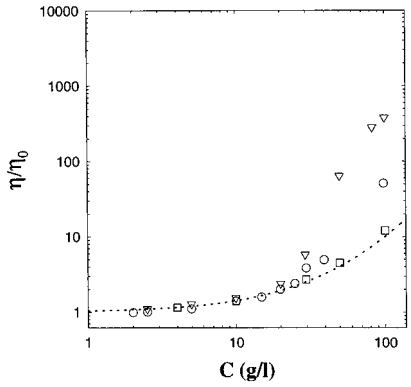

Figure 6. Concentration dependence of the normalized viscosity η/η_0 for α,ω-PEO20 (triangles), ω-PEO20 (circles), and PEO20 (squares). The dotted line represents the results for unmodified PEO.

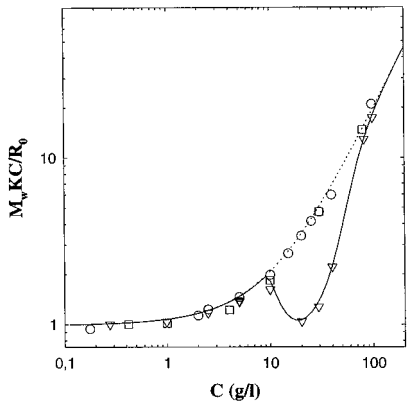

Figure 7. Concentration dependence of M_wKC/R_0 for α,ω-PEO20 (triangles), ω-PEO20 (circles), and PEO20 (squares). The solid line represents the model calculation described in the text. The dotted line represents the results for unmodified PEO.

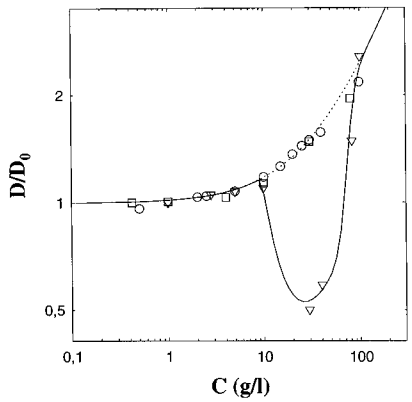

Figure 8. Concentration dependence of D/D_o for α,ω-PEO20 (triangles), ω-PEO20 (circles), and PEO20 (squares). The solid line represents the model calculation with the same values for CAC and for K_0 as used for the calculation shown in Figure 7. The dotted line represents the results for unmodified PEO.

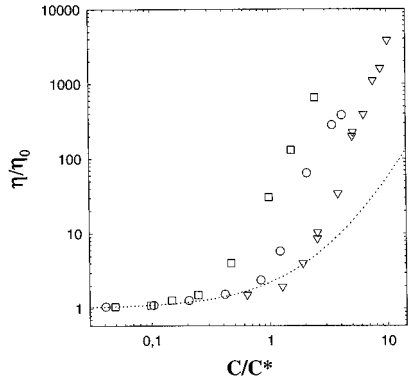

Figure 9. Variation of the normalized viscosity η/η_0 with C/C^* for α,ω-PEO35 (triangles), α,ω-PEO20 (circles), and α,ω-PEO10 (squares). The dotted line represents the results for unmodified PEO.

indistinguishable over the whole concentration range. For the difunctionalized sample, KC/R_0 decreases at concentrations above 9 g/L, which we associate with the critical association concentration. The decrease of KC/R_0 is due to the increase of the weight-average molar mass by the association of α,ω-PEO20 chains above CAC. As the concentration increases further, the increase of M_w is rapidly compensated by interparticle interactions, leading in an increase of KC/R_0. At the highest concentrations KC/R_0 is close to that of unmodified PEO. This is not surprising as KC/R_0 is independent of the molar mass in the semidilute regime if we can neglect the contribution from the small functional groups. The association of ω-PEO20 is completely masked by interactions.

DLS. In Figure 8 the concentration dependence of the normalized apparent diffusion coefficient is shown for α,ω-PEO20, ω-PEO20, and PEO20. The diffusion coefficient at low concentrations is the translation diffusion coefficient of the individual PEO chains: 4.4×10^{-11}, 4.4×10^{-11}, and 5.0×10^{-11} $m^2\ s^{-1}$ for α,ω-PEO20, ω-PEO20, and PEO20, respectively. The DLS results are consistent with the SLS results. ω-PEO20 and PEO20 have the same concentration dependence over the whole concentration range. For α,ω-PEO20 the diffusion coefficient decreases for $C >$ CAC and increases again at higher concentration due to interactions. At concentrations where D decreases, the relaxation time distribution broadens due to increasing polydispersity of the associated PEO chains; see figure 5. At the highest concentrations the relaxation time distribution is narrower and the diffusion coefficient is close to that of unmodified PEO, because in the semidilute regime D is independent of the molar mass. The normalized diffusion coefficient does not depend on the temperature in the range investigated (20−60 °C).

Molar Mass Dependence. We have investigated the association process of α,ω-PEO with molar mass 10, 20, and 35 kg/mol.

Viscosity. In Figure 9, the concentration dependence of the normalized viscosity of α,ω-PEO10, α,ω-PEO20, and α,ω-PEO35 is shown as a function of C/C^*. The dotted line represents the dependence of unmodified PEO, which is independent of the molar mass in this representation. The upward deviation of the viscosity occurs at larger values of C/C^* when the molar mass is increased. Thus for a given functionalization the associative character decreases with increasing molar mass.

SLS. Normalized values of KC/R_0 are plotted in Figure 10 as a function of C/C^* for α,ω-PEO10, α,ω-PEO20, and α,ω-PEO35. The molar masses of the individual PEO chains obtained from low concentration data are 10, 20, and 36 kg/mol for α,ω-PEO10, α,ω-PEO20, and α,ω-PEO35, respectively. The dotted line represents again the dependence of unmodified PEO. The value of C/C^* where KC/R_0 starts to decrease increases with increasing molar mass. The decrease of KC/R_0 is more pronounced at lower molar mass and is small for the highest molar mass. As mentioned above, the decrease is caused by association of the PEO chains and the subsequent increase is due to interactions which

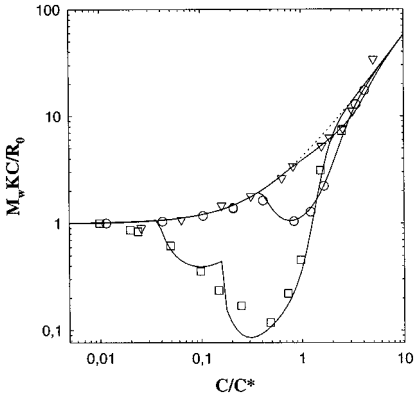

Figure 10. Variation of M_wKC/R_0 with C/C^* for α,ω-PEO35 (triangles), α,ω-PEO20 (circles), and α,ω-PEO10 (squares). The solid lines represent the model calculations described in the text. The dotted line represents the results for unmodified PEO.

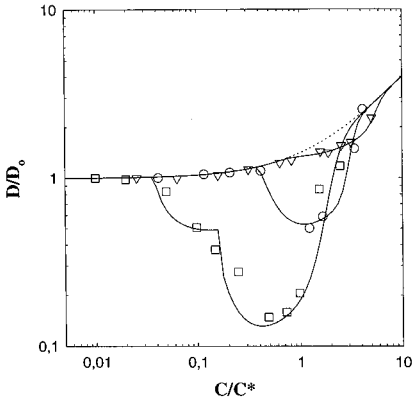

Figure 11. Variation of D/Do with C/C^* for α,ω-PEO35 (triangles), α,ω-PEO20 (circles), and α,ω-PEO10 (squares). The solid lines represent the model calculations described in the text. The dotted line represents the results for unmodified PEO.

become important when the concentration approaches the overlap concentration. If the molar mass is larger the association starts at higher values of C/C^* and interactions mask the effect more strongly. As expected, at the highest concentrations KC/R_0 is independent of the molar mass and close to that of unmodified PEO.

DLS. Figure 11 shows the normalized diffusion coefficient of α,ω-PEO10, α,ω-PEO20, and α,ω-PEO35 as a function of C/C^*. The values of D_0 are 6.7×10^{-11}, 4.4×10^{-11}, and 3.4×10^{-11} m^2 s^{-1} for α,ω-PEO10, α,ω-PEO20, and α,ω-PEO35, respectively. The concentration dependence shows the same features as the SLS results: the association process is more pronounced and begins at lower values of C/C^* for lower molar mass samples.

Discussion

We have seen that the SLS and DLS results on end-functionalized PEO can be understood as a combined effect of association and interactions. The association occurs because the dodecyl groups cluster into multiplets of well defined size. Based on a similar study of telechelic ionomers, we concluded that a two-step association process occurs for that system.[16] At low concentrations the ionomers associate into well defined small clusters containing one multiplet, in a way analogous to the formation of micelles. At higher concentrations, but well below C^* these clusters associate by bridging, i.e., two ends belong to different multiplets. With increasing concentration the aggregates grow with a broadening size distribution. Above a certain concentration, C_{gel}, the clusters form a transient network and the viscosity increases sharply. Ionomers functionalized at one end can only form clusters containing a single multiplet.

A similar association process is expected for modified PEO. The main difference is that the association occurs at much higher concentrations so that the two steps take place simultaneously, except perhaps for α,ω-PEO10, see below. In order to give a more quantitative description of the data, we will use the following crude model. We will assume that the association process can be described by an open association model for which the weight (M_w^a) and number (M_n^a) average molar mass of the aggregates are given by[17]

$$M_w^{a\,2} = (M_w^u)^2\left(1 + 4000K_0\left(\frac{C_a}{M_n^u}\right)\right)$$

$$M_n^a = M_n^u\left(1 + 1000K_0\,\frac{C_a}{M_n^a}\right) \qquad (8)$$

Here M^u is the molar mass of the unimer and K_0 is the equilibrium constant for the association process. The unimer concentration, C_u, is assumed equal to C for $C <$ CAC and equal to CAC at larger concentrations. $C_a = C - C_u$ is the concentration of PEO in the aggregated state and is expressed in weight/volume. The unimer can either be the small cluster formed at very low concentrations as is the case of telechelic ionomers or the single polymer chain if the two association steps are simultaneous as is the case for α,ω-PEO20 and α,ω-PEO35. K_0 is assumed to be independent of the size of the aggregates.

The difficulty is to correctly incorporate interactions. At low concentrations one could use estimates of the second and third virial coefficient for branched polymers as was done in ref 18. However, this procedure is obviously incorrect at concentrations above C^*, and furthermore it is not clear how one can quantify the effect of increasing polydispersity on the virial coefficients. For these reasons we have chosen a different approach and assumed that the concentration dependence of the interactions is the same as for unmodified polymers if the concentration is normalized by C^* of the system. The interaction is then described by F_s given by eq 3. KC/R_0 normalized by the molar mass of the individual PEO chains is calculated as

$$\frac{M_wKC}{R_0} = \frac{M_wC}{(M_w^uC_u + M_w^aC_a)}F_s \qquad (9)$$

To calculate C^* of the system at each concentration, we have used the number-average molar mass and radius of gyration of the system, assuming for simplicity the same relation between M and R_g as for linear PEO. Although the model calculations are not very sensitive to the precise values of C^*, the model is very crude, as the interaction term does not take into account the effect of branching or the large polydispersity of the system.

In addition, the open association model is only a reasonable approximation at the initial stage of the association, as it does not predict a sol−gel transition. The situation is similar to that of cluster−cluster aggregation. Monte-Carlo simulations of irreversible cluster aggregation shows the transition to growth via

Table 2. Characteristics of the Modified PEO Samples

sample	CAC domain,[a] g/L	CAC, g/L	$K_0 \times 10^{-6}$, L/mol of unimer	C_{gel}, g/L
α,ω-PEO35	$3 < C < 60$	10	1	38
α,ω-PEO20	$2 < C < 30$	9	30	24
α,ω-PEO10	$0.46 < C < 6.7$	1.5	20	14

[a] From fluorescence measurements reported in ref 2.

a percolation process close to the gel point.[19] We are currently extending this work to reversible aggregation in the hope to obtain a more realistic description of the structure and size distribution of the aggregates as a function of the concentration. The critical concentration where a transient gel is formed (C_{gel}) can be estimated as the concentration where the viscosity sharply increases and is larger than CAC; see Table 2. The viscosity does not diverge at the gel point because the cross-links have a finite lifetime.

In spite of the crude approximations in the model we can fit for α,ω-PEO20 and α,ω-PEO35 the decrease and the beginning of the subsequent increase of the data with two fit parameters: K_0 and CAC, see Table 2. The values of CAC coincide with the concentration where KC/R_0 starts to decrease and are not really model dependent. CAC values are compatible with those obtained from fluorescence spectroscopy also given in Table 2. We do not think that the equilibrium constants, K_0, have a physical meaning except in the sense that they show that the higher molar mass sample is less associative.

At higher concentrations the model calculations show a more gradual increase than the experimental data. As mentioned above, for concentrations much larger than the overlap concentration of the individual PEO chains, KC/R_0 normalized by the molar mass of the individual PEO chains is expected to be the same if plotted as a function of C/C^*, regardless the molar mass and functionalization of the samples. Experimentally this situation is reached at $C/C^* > 4$ but in the model calculations, it is reached only at much larger values. To describe the data over the whole concentration regime, we have used a simple hybrid of eqs 3 and 9 such that eq 9 dominates at concentrations below the minimum and eq 3 at concentrations above $4C^*$. The results for α,ω-PEO20 and α,ω-PEO35 are well described by using this procedure; see solid lines in Figures 7 and 10.

The method does not work for α,ω-PEO10, as the model predicts a much sharper decrease at CAC than is actually observed. As CAC occurs well below C^* one could invoke the two-step association process mentioned above. Initially at $C \approx 0.04C^*$ small clusters are formed via closed association, which subsequently form the unimers of the open association starting at $C \approx 0.15C^*$. Incorporating this effect in the model, we obtained the solid lines through the α,ω-PEO10 data in Figure 10, where we assumed that the unimers consisted of five PEO chains. The model calculation shows the sharp features of a distinct two-step association process, which is not seen in the Experimental Data. However, it is probable that the nonnegligible polydispersity of the α,ω-PEO10 chains gives rise to more gradual transitions. Fluorescence spectroscopy also shows that the association of the functional groups occurs over a broad concentration range for this sample.

The same model can be used to describe the concentration dependence of the apparent diffusion coefficient. Without interactions one would measure the *z*-average diffusion coefficient. As for the SLS data, we incorporate interactions by assuming that they are the same as for linear PEO given by F_d. The apparent diffusion coefficient normalized by the translation diffusion coefficient of the individual PEO chains is calculated as

$$\frac{D}{D_0} = \frac{M_w^u C_u D_0^u + M_w^a C_a D_0^a}{M_w^u C_u + M_w^a C_a} F_d/D_0 \qquad (10)$$

Here D_0^u is the translation diffusion coefficient of the unimer and D_0^a that of the aggregates. We have calculated D_0^a from M_w^a using the relation between the molar mass and the translation diffusion coefficient for linear PEO given in ref 12. To model the data of α,ω-PEO10, we include again the formation of small clusters as a first step. To describe the data over the whole concentration range, we use a hybrid of eq 10 dominating at low concentrations and eq 5 dominating at high concentrations.

The solid lines in Figures 8 and 11 represent model calculations using the same parameters as were used to describe the SLS results. The good agreement shows that the DLS results are consistent with the SLS results and demonstrates that the model, however crude, captures the main features of the aggregation process.

As mentioned above, the viscosity does not diverge at C_{gel} because the cross-links have a finite lifetime. The viscosity of the transient gel is proportional to the lifetime of the functional group in the multiplet. At concentrations above the entanglement concentration unfunctionalized polymers also form a transient network in which the entanglements act as cross-links. The effect of association on the viscosity remains significant as long as the lifetime of the entanglements is smaller than that of the functional group in the multiplet. The disentanglement time increases strongly with increasing concentration, while the lifetime of the functional group in the multiplet is not expected to depend on the overall concentration. This means that at large values of C/C^* the effect of association becomes small for weakly associating polymers such as modified PEO with high molar mass.

Conclusion

Aqueous PEO solutions contain a small amount of large aggregates at all concentrations investigated. These spurious aggregates are present in both modified and unmodified PEO solutions. The amount of material involved in these spurious aggregates is very small and can easily be removed by filtration in the case of unmodified PEO solutions. In the case of modified PEO solutions we were not able to completely remove the spurious aggregates, but their influence on the experimental results can be taken into account by combination of static and dynamic light scattering.

PEO end-capped with dodecyl groups associates when dissolved in water at concentrations above CAC. CAC increases strongly with increasing molar mass in the range investigated, see Table 2. The experimental results are consistent with an initial association according to an open association model followed by percolation type growth to form a transient gel. The extent to which the association is visible in SLS and DLS experiment depends on CAC. If CAC is much smaller than the overlap concentration of the PEO chains, the effect is strong; if it is much larger, the effect is masked by interparticle interactions. A crude model that incorporates these interactions describes the data well.

The smallest PEO investigated showed signs of a two-step association process: first association into well defined small clusters which at higher concentrations aggregate according to an open association model. Contrary to the case of telechelic ionomers, the two steps are not very distinct, possibly due to the polydispersity of the sample. The two steps occur simultaneously for the higher molar mass PEO samples.

Viscosity measurements show that PEO end-capped on only one end also associates. The aggregates formed are necessarily small as the second step in the association of difunctionalized PEO is not possible for monofunctionalized PEO. For the sample investigated, the effect on the SLS and DLS measurements is masked by interactions.

Acknowledgment. This work has been supported by the CPR CNRS DIMAT. We acknowledge stimulating discussions in the framework of this program and we thank J. François and co-workers for providing the samples.

References and Notes

(1) François, J. *Prog. Org.Coat.* **1994**, *24*, 67.
(2) *Hydrophobic Polymers*; Alami, E., Rawiso, M., Isel, F., Beinert, G., Binana-Limbele, W., François, J., Eds.; Advances in Chemistry Series 248; American Chemical Society: Washington, DC, 1995; Chapter 18.
(3) Alami, E.; Almgren, M.; Brown, W.; François, J. *Macromolecules* **1996**, *29*, 2229.
(4) Abrahmsén-Alami, S. Ph.D. dissertation, Stockholm 1996.
(5) Abrahmsén-Alami, S.; Stilbs, P. *J. Phys. Chem.* **1994**, *98*, 6359.
(6) Abrahmsén-Alami, S.; Persson, K.; Stilbs, P.; Alami, E. *J. Phys. Chem.* **1996**, *100*, 4598.
(7) François, J.; Maître, S. Private Communication.
(8) Berne, B.; Pecora, R. *Dynamic Light Scattering*; Wiley: New York, 1976.
(9) Stepanek, P. In *Dynamic Light Scattering*; Brown, W., Ed.; Oxford University Press: Oxford, 1993; Chapter 4.
(10) Porsch, B.; Sundelöf, L. O. *Macromolecules* **1995**, *28*, 7165.
(11) Huglin, M. B., Ed. *Light scattering from polymer solutions*; Academic Press: London and New York, 1972.
(12) Devanand, K.; Selser, J. C. *Macromolecules* **1991**, *24*, 5943. Selser, J. In *Light scattering: principles and development*; Brown, W., Ed.; Oxford University Press: Oxford, 1996; Chapter 7.
(13) de Gennes, P.-G. *Scaling concepts in polymer physics*; Cornell University Press: Ithaca, NY, 1979. Doi, M.; Edwards, S. F. *The theory of polymer dynamics*; Clarendon Press: Oxford, 1986. Brown, W.; Nicolai, T. *Dynamic Light Scattering*; Brown, W., Ed.; Oxford University Press: Oxford, 1993; Chapter 6.
(14) de Gennes, P.-G. *Macromolecules* **1976**, *9*, 587. Adam, M.; Delsanti, M.; *J. Phys.* **1983**, *44*, 1185.
(15) Fetters, L. J.; Lohse, D. J.; Richter, D.; Witten, T. A.; Zirkel, A. *Macromolecules* **1994**, *27*, 4640.
(16) Chassenieux, C.; Johannsson, R.; Durand, D.; Nicolai, T.; Vanhoorne P.; Jérôme R. *Colloids Surf. A* **1996**, *112*, 155.
(17) Elias, H. G. In *Light scattering from polymer solutions*; Huglin, M. B., Ed.; Academic Press: London and New York, 1972; Chapter 9.
(18) Merkle, G.; Burchard, W. *Macromolecules* **1996**, *29*, 5734.
(19) Gimel, J. C.; Durand, D.; Nicolai, T. *Phys. Rev. B* **1995**, *51*, 11348.

MA970354J